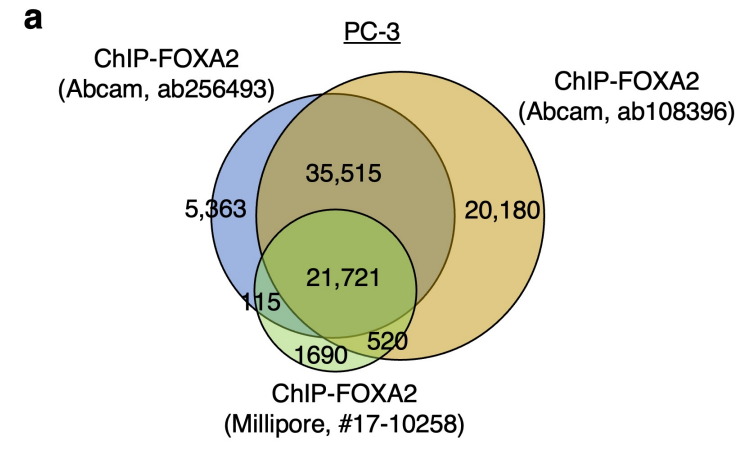
a
PC-3
ChIP-FOXA2
(Abcam, ab256493)
ChIP-FOXA2
(Abcam, ab108396)
ChIP-FOXA2
(Millipore, #17-10258)
5,363
35,515
20,180
21,721
115
1690
520

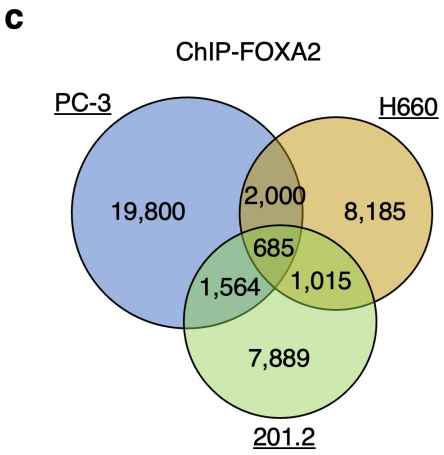
c
ChIP-FOXA2
PC-3
H660
201.2
19,800
2,000
8,185
685
1,564
1,015
7,889

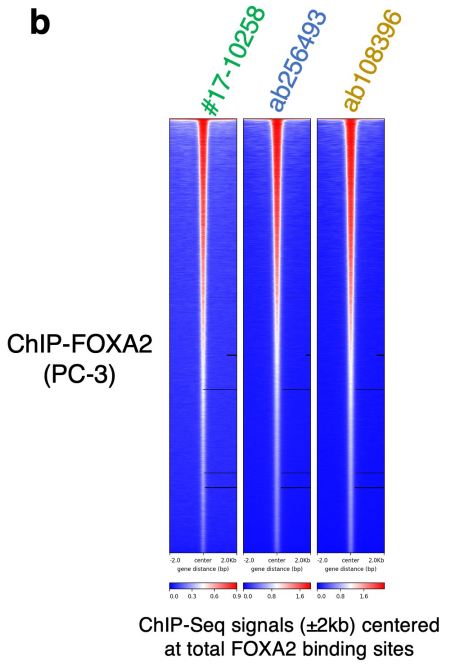
b
#17-10258
ab256493
ab108396
ChIP-FOXA2
(PC-3)
ChIP-Seq signals (±2kb) centered
at total FOXA2 binding sites

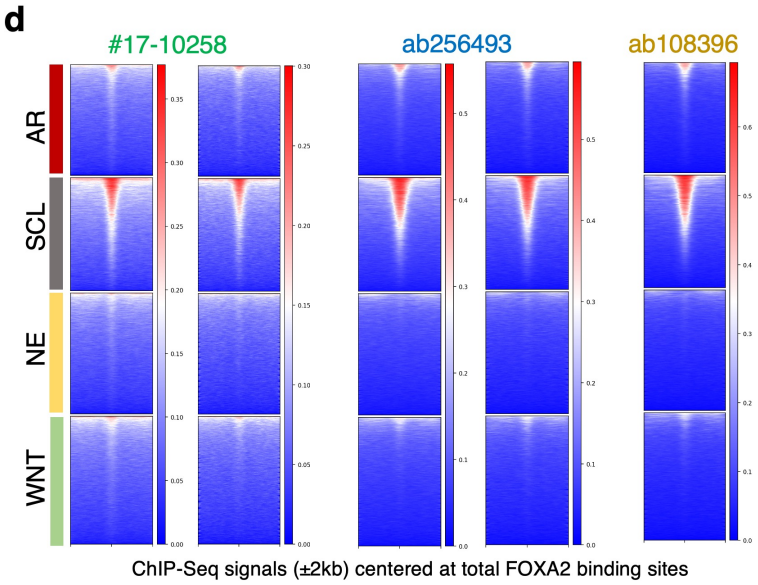
d
#17-10258
ab256493
ab108396
AR
SCL
NE
WNT
ChIP-Seq signals (±2kb) centered at total FOXA2 binding sites

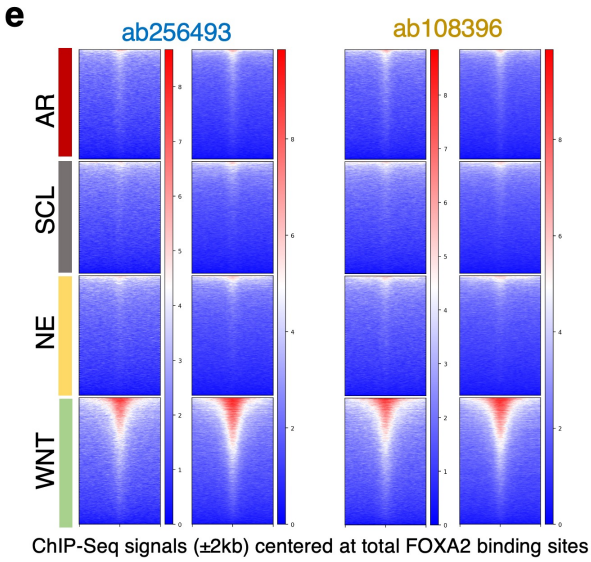
e
ab256493
ab108396
AR
SCL
NE
WNT
ChIP-Seq signals (±2kb) centered at total FOXA2 binding sites

Supplementary Fig. 1| FOXA2 cistrome in PCa models

a, ChIP-seq analyses of FOXA2 were conducted in PC-3 cells with indicated commercially available ChIP-grade antibodies. The Venn diagram shows the overlap of binding sites. **b**, Heatmap view for the FOXA2 binding intensity at all those sites, indicating consistent chromatin binding profiles from all three antibodies. **c,** The Venn diagram view for FOXA2 ChIP-seq peaks in PC-3, NCI-H660, and 201.2 models. **d**, **e**, Heatmap view for the FOXA2 binding intensity at lineage-specific ATAC-signature sites [1] using three different antibodies with additional replicates for PC-3 cells (d) and two different antibodies for 201.2 tumor samples (e).

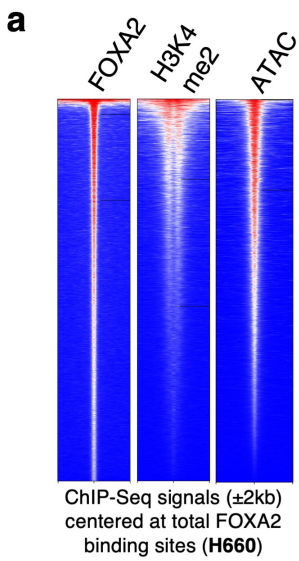

b

Mass-spectrometry

Rep1/Rep2(Methyl)
R208me, R208me2
R228me
K265me, K265me2
K270me2
K280me, K280me2
K321me, K321me2

Supplementary Fig. 2| FOXA2 binds to enhancers marked by high levels of H3K4me2 and ATAC signal

a, Heatmap view for FOXA2, H3K4me2, and ATAC (Assay for Transposase-Accessible Chromatin using sequencing) peaks in NCI-H660 cells centered at the FOXA2 sites in NCI-H660. **b,** Mass-spectrometry analysis was performed on immunoprecipitated FLAG-FOXA2 in PC3 cells stably overexpressing FLAG-tagged FOXA2. Methylation sites on various FOXA2 amino acids were consistently detected in two biological replicates (K265 methylation highlighted in yellow).

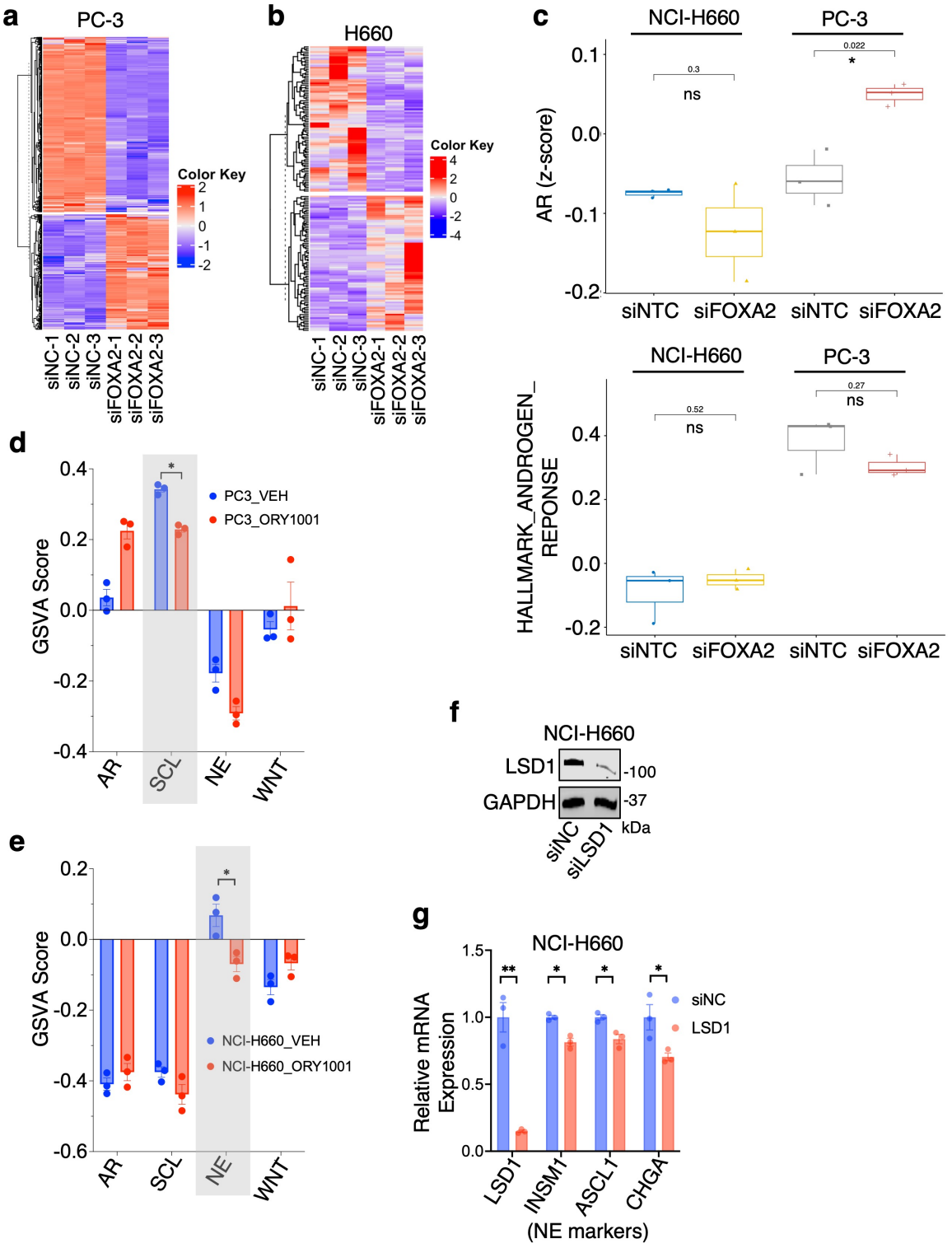

Supplementary Fig. 3| FOXA2 transcriptome in PC-3 and NCI-H660 models

a, **b**, Heatmap view for RNA-seq data showing the expression levels of FOXA2-upregulated/downregulated genes (log_2(fold-change) > 1, $P < 0.05$) in PC3 cells (a) and NCI-H660 cells (b) transfected with siFOXA2 versus

siNTC. **c**, Box plot for AR expression (upper panel) and Hallmark androgen response gene signature scores (lower panel, d) in PC-3/NCI-H660 cells transfected with siFOXA2 versus siNTC (n=3 independent samples; center: median; box: 25th to 75th IQR; whiskers: 1.5x IQR; outliers: individual data points; statistical significance determined by unpaired two-sided *t*-test). **d**, **e**, GSVA scores for subtype-specific transcriptional signatures (based on gene annotation nearby lineage-specific ATAC signature sites [1]) in PC3 cells (d) or NCI-H660 cells (e) treated with/out LSD1 inhibitor, ORY1001 (n=3 independent samples; data represented as mean ± SEM; statistical significance determined by unpaired two-sided *t*-test). **f**, Immunoblotting for LSD1 in NCI-H660 cells transfected by siNTC or siLSD1 (n=3 independent experiments). **g**, qRT-PCR for indicated genes in these cells (n=3 independent samples; data represented as mean ± SEM; statistical significance determined by unpaired two-sided *t*-test). ns (P>0.05), * (0.01<P<0.05), ** (0.001<P<0.01), *** (P<0.001), and **** (P<0.0001) were used to indicate the levels of *P*-value. Source data are provided as a Source Data file.

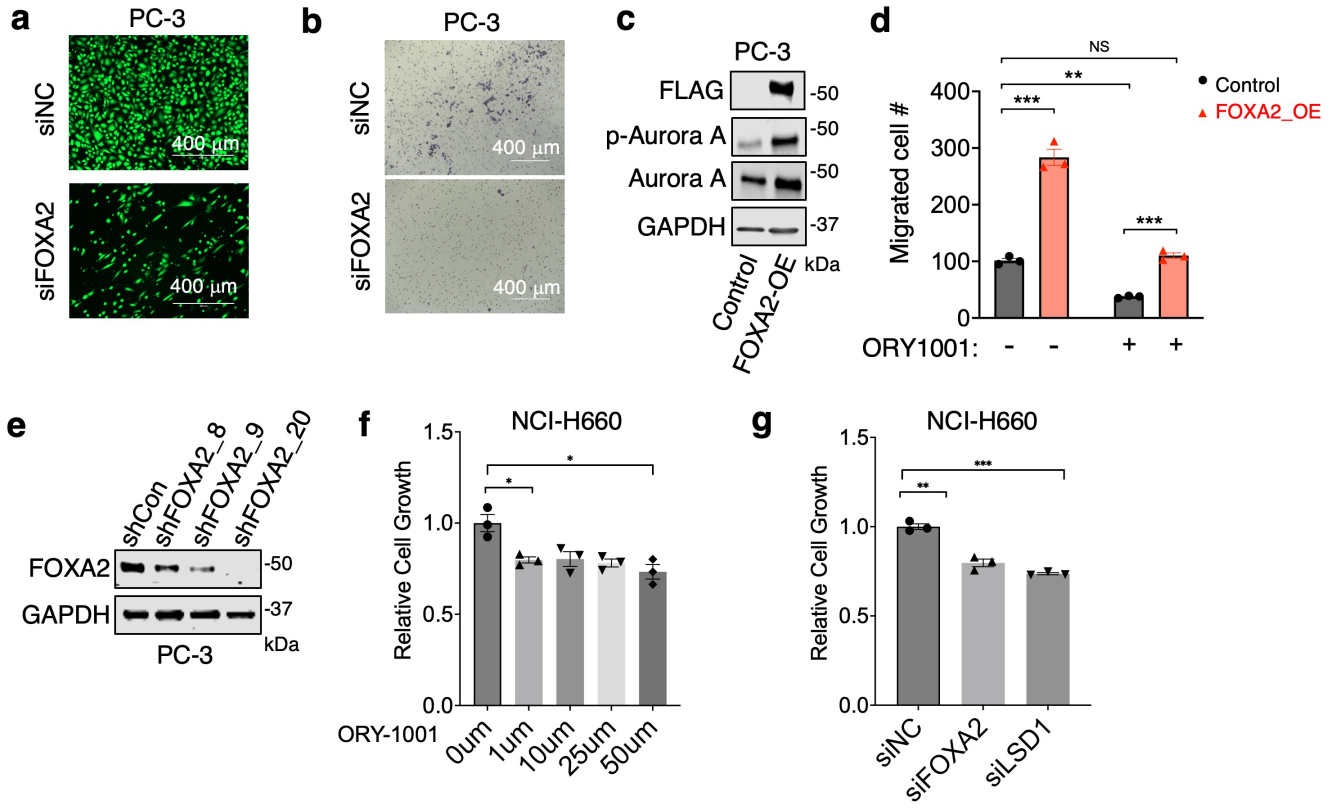

Supplementary Fig. 4| FOXA2 promotes CRPC tumor progression

a, **b**, Transwell migration assay (a) or Boyden chamber invasion assay (b) in PC-3 cells transfected with siFOXA2 versus siNTC. **c**, Immunoblotting for indicated proteins in PC-3 cells stably overexpressing FOXA2 (FOXA2-OE) versus control stable cells (n=3 independent experiments). **d**, Transwell migration assay in control PC-3 or PC-3-FOXA2-OE cells treated with /out ORY-1001 (10μM for 2d) (n=3 independent samples; data represented as mean ± SEM; statistical significance determined by unpaired two-sided *t*-test). **e**, Immunoblotting for FOXA2 in PC-3 cells stably infected with three lentiviral shRNAs against FOXA2 versus non-target-control (NTC) (n=3 independent experiments). **f**, **g**, Proliferation assay for NCI-H660 cells treated with ORY-1001 (10μM for 3d) (f) or transfected with siFOXA2 or siLSD1 (g) (n=3 independent samples; data represented as mean ± SEM; statistical significance determined by unpaired two-sided *t*-test). ns ($P>0.05$), * ($0.01<P<0.05$), ** ($0.001<P<0.01$), *** ($P<0.001$), and **** ($P<0.0001$) were used to indicate the levels of *P*-value. Source data are provided as a Source Data file.

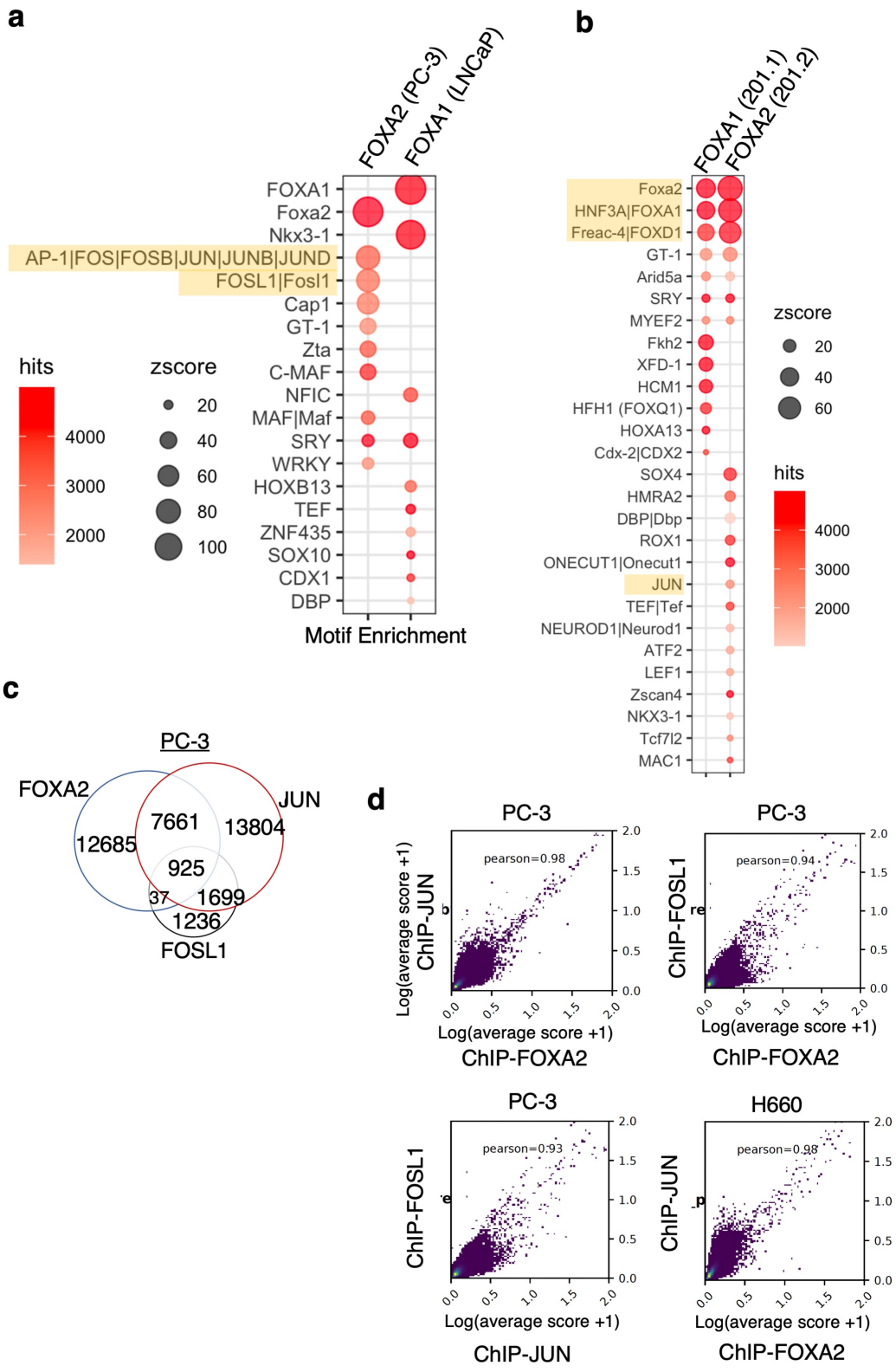

Supplementary Fig. 5| FOXA2 and JUN chromatin binding sites are highly correlated

a, **b**, Motifs enrichment analyses for ChIP-FOXA2 sites in PC-3 and ChIP-FOXA1 sites in LNCaP cells (a) or

201.1 and 201.2 tumor samples (b) by SeqPos motif tool. **c**, Venn diagram for FOXA2, JUN, or FOSL1 binding sites in PC-3 cells. **d,** A scatterplot for the correlation between two indicated ChIP-seq profiles based on read coverage within genomic regions using a bin size of 5kb in PC-3 and NCI-H660 cells. Pearson correlation coefficient was calculated. multiBigwigSummary and plotCorrelation tools were used for this analysis.

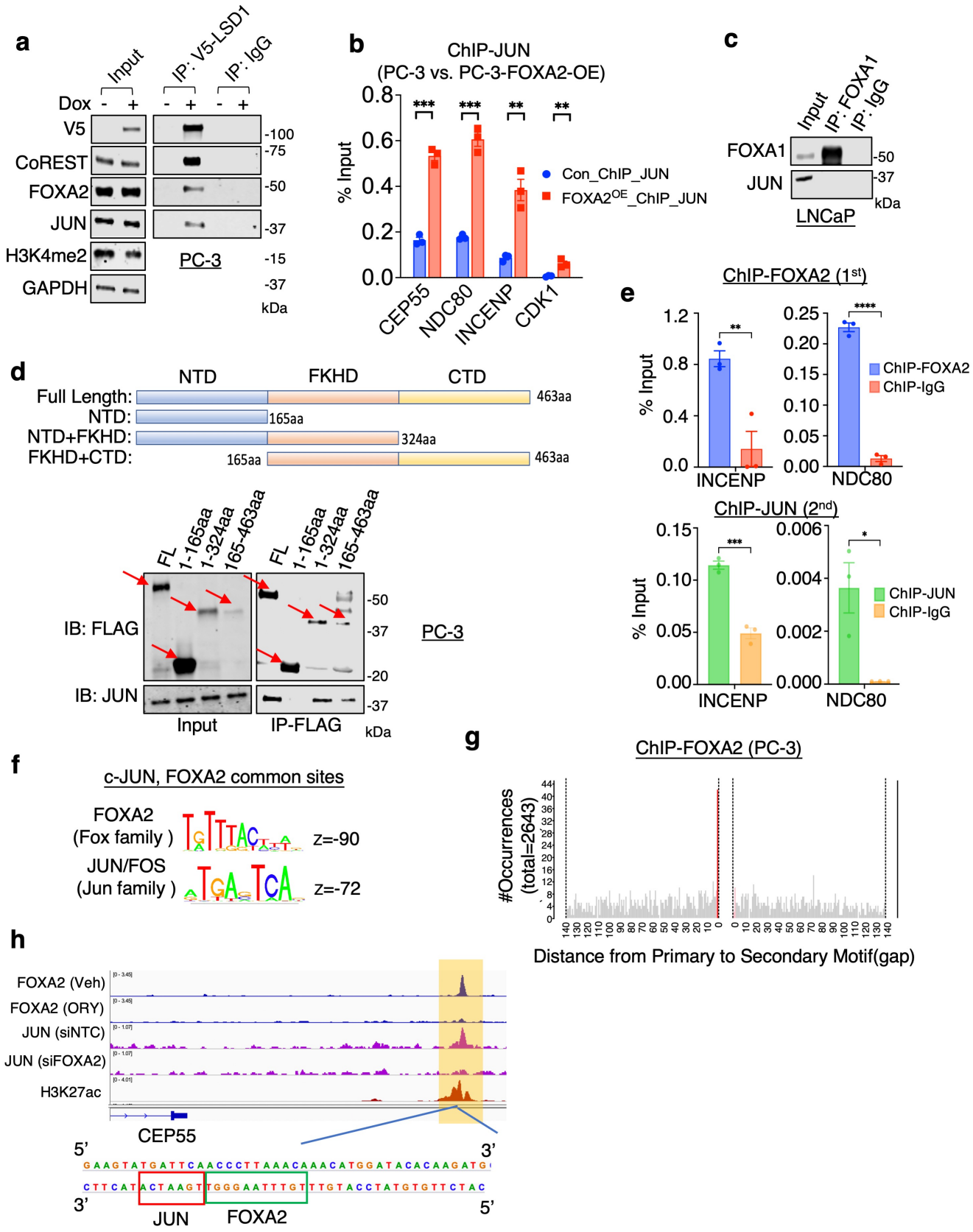
a
Input
IP: V5-LSD1
IP: IgG
Dox - + - + - +
V5
CoREST
FOXA2
JUN
H3K4me2
GAPDH
PC-3
-100
-75
-50
-37
-15
-37
kDa
b
ChIP-JUN
(PC-3 vs. PC-3-FOXA2-OE)
% Input
0.8
0.6
0.4
0.2
0.0
***
***
**
**
Con_ChIP_JUN
FOXA2OE_ChIP_JUN
CEP55
NDC80
INCENP
CDK1
c
Input
IP: FOXA1
IP: IgG
FOXA1
JUN
-50
-37
kDa
LNCaP
d
NTD
FKHD
CTD
Full Length:
NTD:
NTD+FKHD:
FKHD+CTD:
463aa
165aa
324aa
165aa
463aa
FL
1-165aa
1-324aa
165-463aa
IB: FLAG
IB: JUN
-50
-37
-20
-37
kDa
Input
IP-FLAG
PC-3
e
ChIP-FOXA2 (1st)
% Input
1.2
0.8
0.4
0.0
**
INCENP
0.25
0.20
0.15
0.10
0.05
0.00
****
NDC80
ChIP-FOXA2
ChIP-IgG
ChIP-JUN (2nd)
0.15
0.10
0.05
0.00
***
INCENP
0.006
0.004
0.002
0.000
*
NDC80
ChIP-JUN
ChIP-IgG
f
c-JUN, FOXA2 common sites
FOXA2
(Fox family)
z=-90
JUN/FOS
(Jun family)
z=-72
g
ChIP-FOXA2 (PC-3)
#Occurrences
(total=2643)
Distance from Primary to Secondary Motif(gap)
h
FOXA2 (Veh)
FOXA2 (ORY)
JUN (siNTC)
JUN (siFOXA2)
H3K27ac
CEP55
5'
3'
GAAGTATGATTCAACCCTTAAACAAACATGGATACACAAGATG
CTTCATACTAAGTTGGGAATTTGTTTGTACCTATGTGTTCTAC
3'
5'
JUN
FOXA2

Supplementary Fig. 6| FOXA2 interacts with JUN on chromatin

a, Immunoblotting for indicated proteins that were co-immunoprecipitated with V5 in PC-3 stable cells overexpressing doxycycline-inducible V5-tagged LSD1 (treated with 0.5ug/ml doxycycline to induce LSD1 overexpression, n=3 independent experiments) . **b,** ChIP-qPCR for validating the binding of JUN at the identified FOXA2 target sites in PC-3 cells stably overexpressing FOXA2 (n=3 independent samples; data represented as mean ± SEM; statistical significance determined by unpaired two-sided *t*-test). **c,** Immunoblotting for indicated proteins that were co-immunoprecipitated with FOXA1 in LNCaP cells (n=3 independent experiments). **d,** Immunoblotting for indicated proteins that were co-immunoprecipitated with FLAG in PC-3 cells transiently expressing FLAG-tagged truncated FOXA2 proteins (n=3 independent experiments). **e,** ChIP-qPCR to validate the co-occupancy of FOXA2 and JUN on the indicated FOXA2 target sites PC-3 cells using a re-ChIP sequential approach with FOXA2 and JUN antibodies (n=3 independent samples; data represented as mean ± SEM; statistical significance determined by unpaired two-sided *t*-test). **f**-**h**, Motif enrichment analysis was performed at FOXA2 and JUN co-binding sites in PC-3 cells to identify the top-ranked enriched motifs (f), followed by the analysis of the distance from the primary to the secondary motif (gap) for composition motif enrichment (g) and a genome browser view for a FOXA2/JUN co-binding site at *CEP55* gene loci (h). ns ($P>0.05$), * ($0.01<P<0.05$), ** ($0.001<P<0.01$), *** ($P<0.001$), and **** ($P<0.0001$) were used to indicate the levels of *P*-value. Source data are provided as a Source Data file.

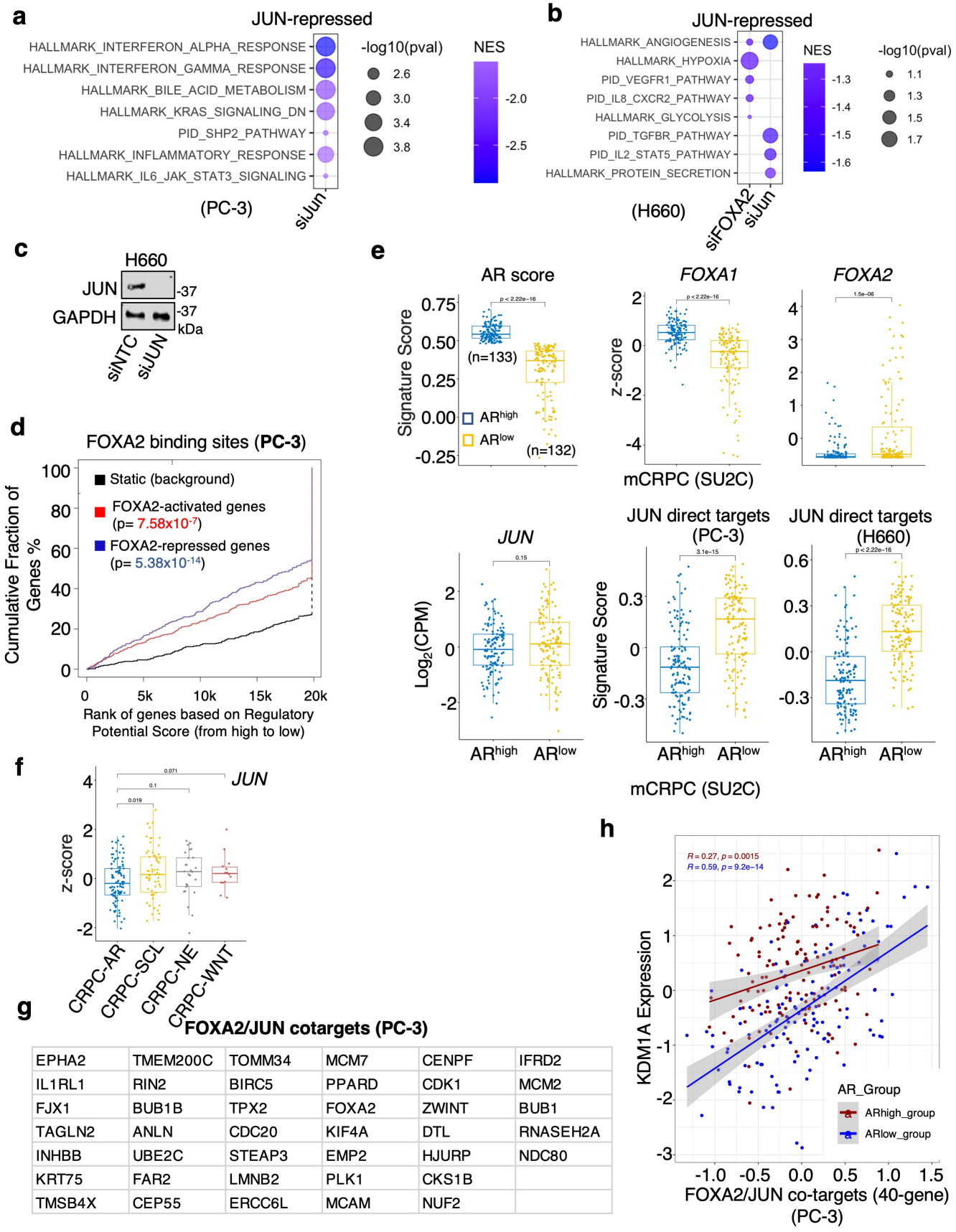

EPHA2	TMEM200C	TOMM34	MCM7	CENPF	IFRD2
IL1RL1	RIN2	BIRC5	PPARD	CDK1	MCM2
FJX1	BUB1B	TPX2	FOXA2	ZWINT	BUB1
TAGLN2	ANLN	CDC20	KIF4A	DTL	RNASEH2A
INHBB	UBE2C	STEAP3	EMP2	HJURP	NDC80
KRT75	FAR2	LMNB2	PLK1	CKS1B	
TMSB4X	CEP55	ERCC6L	MCAM	NUF2	

Supplementary Fig. 7| Chromatin binding, expression, and targets of JUN in AR-low CRPC

a, **b**, GSEA using HALLMARK and PID datasets to compare siJUN versus siNTC in PC-3 cells (a) or siJUN and siFOXA2 versus siNTC in NCI-H660 cells (b). **c,** Immunoblotting for JUN in NCI-H660 cells transfected with siJUN versus siNTC (n=3 independent experiments). **d,** BETA integrating ChIP-FOXA2 binding sites and RNA-seq data from PC-3 cells transfected with siNTC versus siFOXA2. **e,** Boxplots (center: median; box: 25th to 75th IQR; whiskers: 1.5x IQR; outliers: individual data points; statistical significance determined by unpaired two-sided *t*-test) for expression scores or levels of AR score, *FOXA1*, *FOXA2*, *JUN*, and JUN-direct-targets (identified from PC-3 or NCI-H660) in AR score-high (n=133) and AR-score low (n=132) CRPC patient samples (SU2C) [2]. **f,** JUN mRNA expression (z-score) in four different CRPC subtypes (CRPC-AR n=104 gens, CRPC-SCL n=62 genes, CRPC-NE n=26, and CRPC-WNT n=14) [1] using the SU2C dataset (center: median; box: 25th to 75th IQR; whiskers: 1.5x IQR; outliers: individual data points; statistical significance determined by unpaired two-sided *t*-test). **g**, **h**, FOXA2/JUN directly regulated co-targets (identified from PC3 cells, g) were correlated with *LSD1* (*KDM1A*) expression in AR score-high versus AR core-low CRPC-AR low CRPC samples (h).

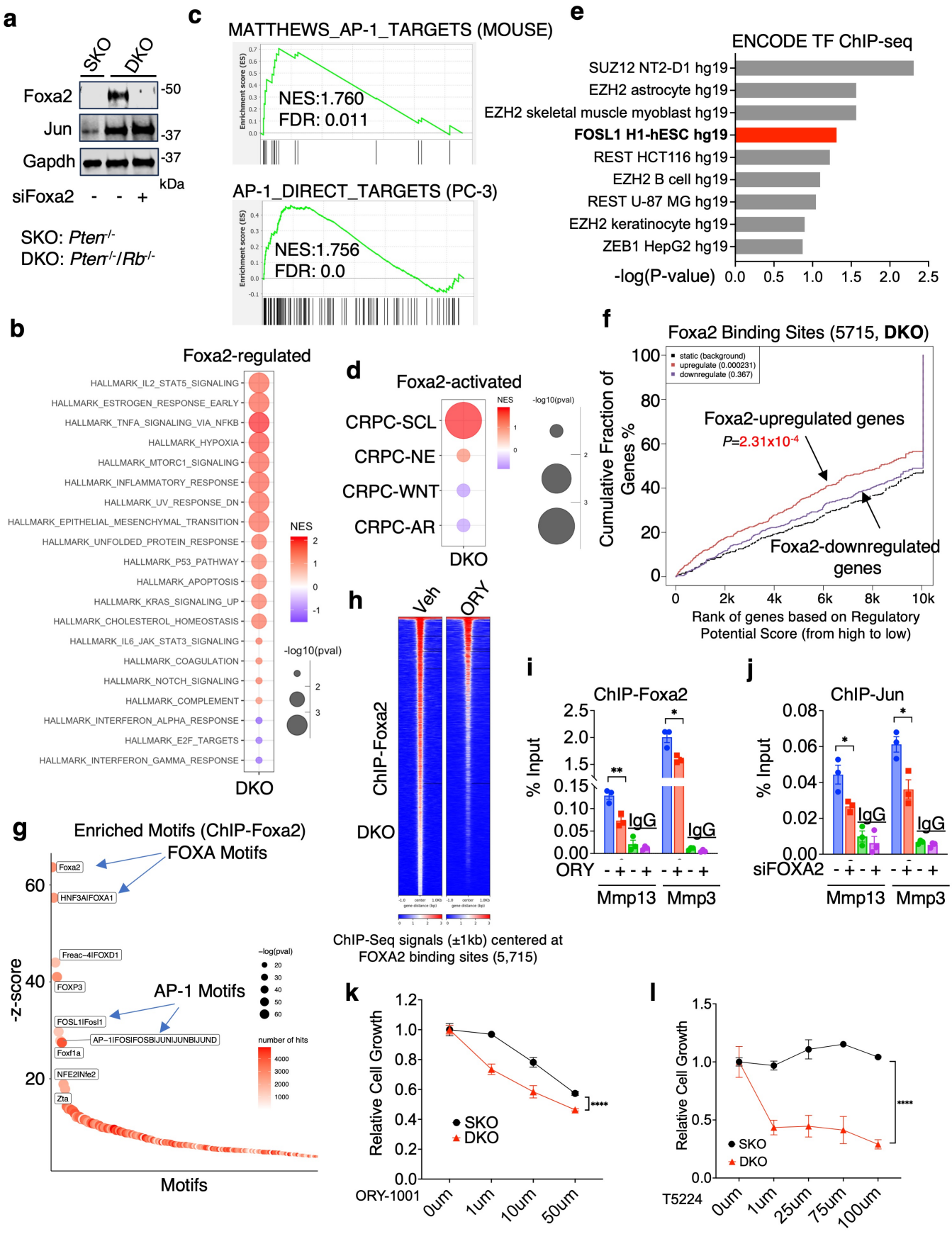
a
SKO
DKO
Foxa2
Jun
Gapdh
-50
-37
-37
kDa
siFoxa2 - - +
SKO: Pten-/-
DKO: Pten-/-/Rb-/-
c
MATTHEWS_AP-1_TARGETS (MOUSE)
NES:1.760
FDR: 0.011
AP-1_DIRECT_TARGETS (PC-3)
NES:1.756
FDR: 0.0
Enrichment score (ES)
e
ENCODE TF ChIP-seq
SUZ12 NT2-D1 hg19
EZH2 astrocyte hg19
EZH2 skeletal muscle myoblast hg19
FOSL1 H1-hESC hg19
REST HCT116 hg19
EZH2 B cell hg19
REST U-87 MG hg19
EZH2 keratinocyte hg19
ZEB1 HepG2 hg19
-log(P-value) 0.0 0.5 1.0 1.5 2.0 2.5
b
Foxa2-regulated
HALLMARK_IL2_STAT5_SIGNALING
HALLMARK_ESTROGEN_RESPONSE_EARLY
HALLMARK_TNFA_SIGNALING_VIA_NFKB
HALLMARK_HYPOXIA
HALLMARK_MTORC1_SIGNALING
HALLMARK_INFLAMMATORY_RESPONSE
HALLMARK_UV_RESPONSE_DN
HALLMARK_EPITHELIAL_MESENCHYMAL_TRANSITION
HALLMARK_UNFOLDED_PROTEIN_RESPONSE
HALLMARK_P53_PATHWAY
HALLMARK_APOPTOSIS
HALLMARK_KRAS_SIGNALING_UP
HALLMARK_CHOLESTEROL_HOMEOSTASIS
HALLMARK_IL6_JAK_STAT3_SIGNALING
HALLMARK_COAGULATION
HALLMARK_NOTCH_SIGNALING
HALLMARK_COMPLEMENT
HALLMARK_INTERFERON_ALPHA_RESPONSE
HALLMARK_E2F_TARGETS
HALLMARK_INTERFERON_GAMMA_RESPONSE
NES
-log10(pval)
DKO
d
Foxa2-activated
CRPC-SCL
CRPC-NE
CRPC-WNT
CRPC-AR
NES
-log10(pval)
DKO
f
Foxa2 Binding Sites (5715, DKO)
static (background)
upregulate (0.000231)
downregulate (0.367)
Foxa2-upregulated genes
P=2.31x10-4
Foxa2-downregulated genes
Cumulative Fraction of Genes %
Rank of genes based on Regulatory Potential Score (from high to low)
h
Veh
ORY
ChIP-Foxa2
DKO
ChIP-Seq signals (±1kb) centered at FOXA2 binding sites (5,715)
i
ChIP-Foxa2
% Input
IgG
ORY - + - + - + - +
Mmp13 Mmp3
j
ChIP-Jun
% Input
IgG
siFOXA2 - + - + - + - +
Mmp13 Mmp3
g
Enriched Motifs (ChIP-Foxa2)
FOXA Motifs
AP-1 Motifs
Foxa2
HNF3A|FOXA1
Freac-4|FOXD1
FOXP3
FOSL1|Fosl1
AP-1|FOS|FOSB|JUN|JUNB|JUND
Foxf1a
NFE2|Nfe2
Zta
-log(pval)
number of hits
-z-score
Motifs
k
Relative Cell Growth
SKO
DKO
****
ORY-1001
0um 1um 10um 50um
l
Relative Cell Growth
SKO
DKO
****
T5224
0um 1um 25um 75um 100um

Supplementary Fig. 8| FOXA2 transcription activity in DKO murine PCa cell line

a, Immunoblotting for Foxa2 and Jun in SKO (*Pten*$^{-/-}$) and DKO (*Pten*$^{-/-}$/*Rb*$^{-/-}$) murine PCa cells transfected with siFoxa2 versus siNTC (n=3 independent experiments). **b**, GSEA using HALLMARK and PID datasets to identify Foxa2 upregulated (siFoxa2-downregulated, red) and downregulated genes (siFoxa2-upregulated, blue). **c**, GSEA for the enrichment of Foxa2 regulated genes using MATTHEWS_AP-1_TARGETS (identified from mouse models) and our AP-1 direct targets (identified from PC-3 model) gene sets. **d,** GSEA for Foxa2-activated genes using lineage-specific signature gene sets. **e**, Prediction of potential transcription factor (TF) regulation for Foxa2-activated genes based on their nearby TF binding peaks using ENCODE TF ChIP-seq database. **f,** ChIP-seq of Foxa2 in DKO cells identified 5,715 peaks (using the antibody ab256493 from Abcam). BETA integrating ChIP-Foxa2 binding sites and RNA-seq data from DKO cells transfected with siNTC versus siFoxa2. **g**, Motif enrichment analysis of Foxa2 binding sites. **h**, ChIP-seq of Foxa2 in DKO cells treated with LSD1 inhibitor (ORY-1001, 10μM, 4h). Heatmap view for the change of Foxa2 binding intensity at 5,715 Foxa2 binding sites. **i**, ChIP-qPCR for Foxa2 binding at two Foxa2 binding sites located at Mmp3 and Mmp13 genes in DKO cells treated with/out ORY-1001 (10μM, 4h) (n=3 independent samples; data represented as mean ± SEM; statistical significance determined by unpaired two-sided *t*-test). **j** ChIP-qPCR for Jun binding at these two sites in DKO cells transfected with siNTC or siFoxa2 (n=3 independent samples; data represented as mean ± SEM; statistical significance determined by unpaired two-sided *t*-test). **k**, **l**, Viability assay for SKO and DKO cells treated with 0-50μM ORY-1001 (k) or 0-100μM T5224 (l) for 3d (n=3 independent samples; data represented as mean ± SEM; statistical significance determined by two-way ANOVA). Note: SKO (*Pten*$^{-/-}$) murine PCa cell line and DKO (*Pten*$^{-/-}$/*Rb*$^{-/-}$) murine PCa cells were cultured in DMEM supplemented with 10% FBS. ns (P>0.05), * (0.01<P<0.05), ** (0.001<P<0.01), *** (P<0.001), and **** (P<0.0001) were used to indicate the levels of P-value. Source data are provided as a Source Data file.

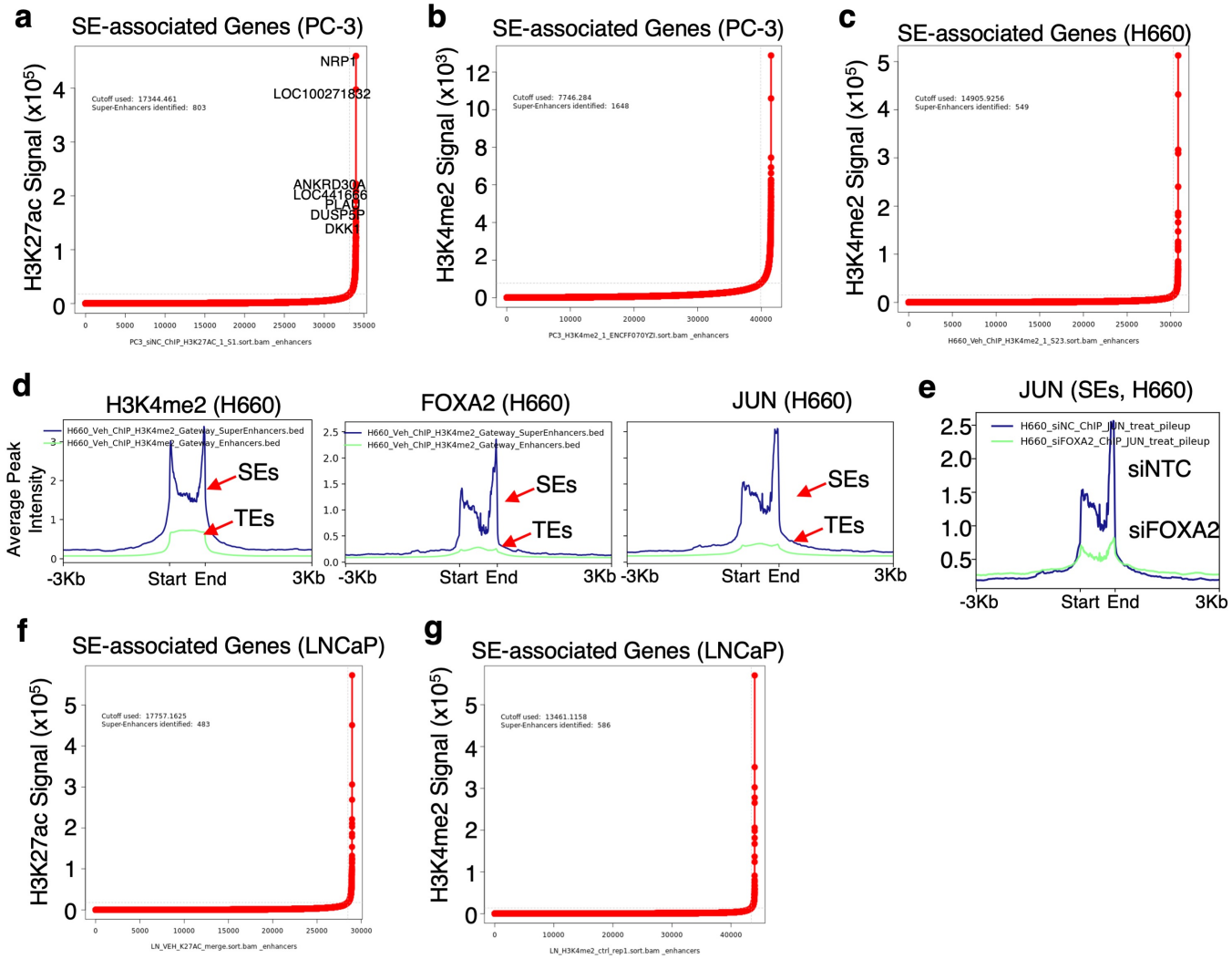

Supplementary Fig. 9| Identification of super-enhancers in different PCa cell lines

a-**c**, Model-specific super-enhancers (SEs) were identified using the ROSE algorithm based on ChIP-seq data for H3K27ac (a) and H3K4me2 (b) in PC3 cells, or H3K4me2 in NCI-H660 cells (c). **d**, Average binding intensity of indicated proteins at super-enhancers (SEs) versus typical enhancers (TEs) in NCI-H660 cells. **e**, Average JUN binding intensity at SEs in NCI-H660 cells transfected with siFOXA2 versus siNTC. **f**, **g**, Super-enhancers were identified using the ROSE algorithm based on ChIP-seq data for H3K27ac (f) and H3K4me2 (g) in LNCaP cells (GSE114268 [3]).

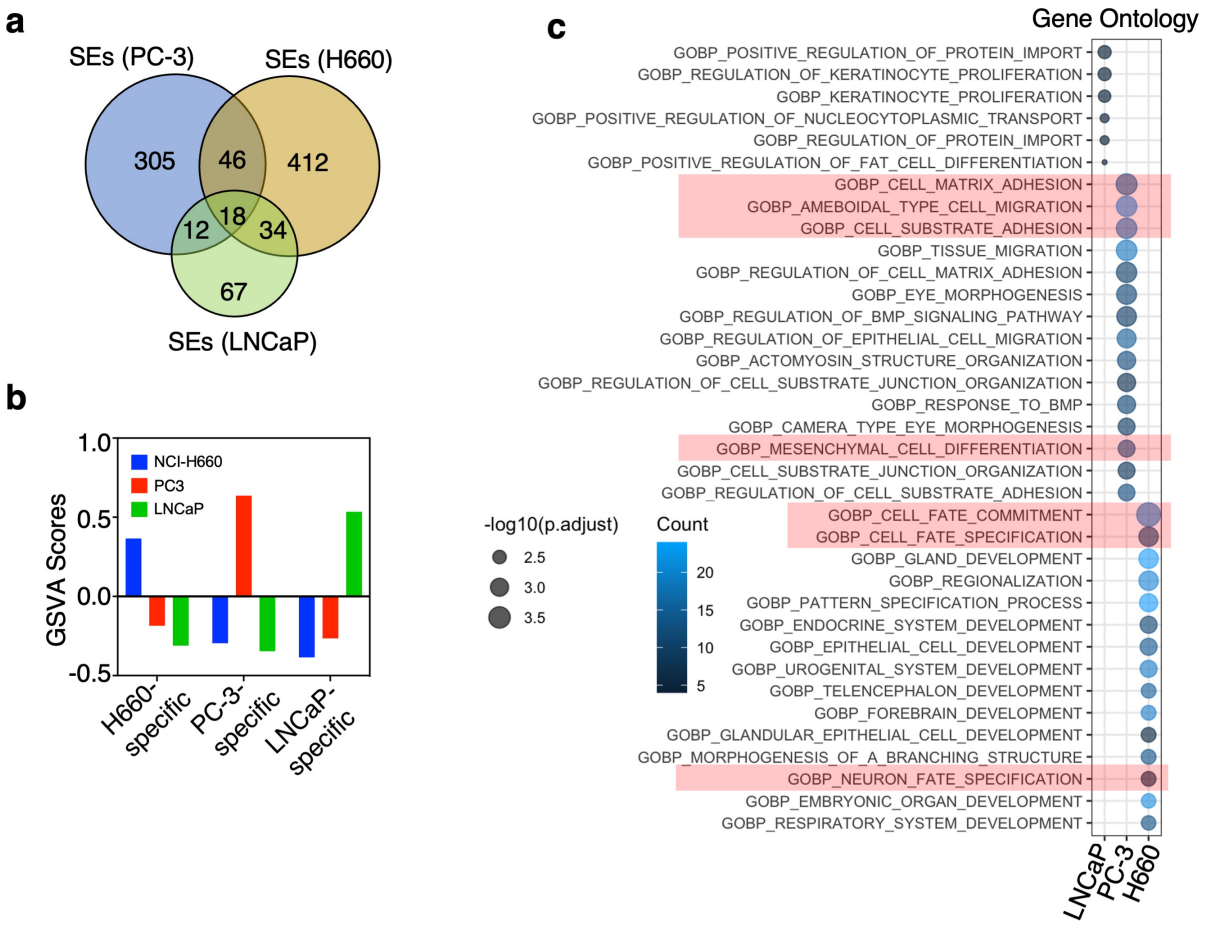

Supplementary Fig. 10| Super-enhancer-associated genes are functionally distinct in CRPC subtypes

a, Venn diagram for super-enhancer (SE)-associated genes in LNCaP, PC3, and H660 cells. **b,** Gene set variation analysis (GSVA) scores of the specific SE-associated genes in LNCaP, PC3, and H660 cells. **c,** Gene ontology annotation analysis to examine the functional enrichment of SE-associated genes identified in LNCaP, PC3, and H660 cells.

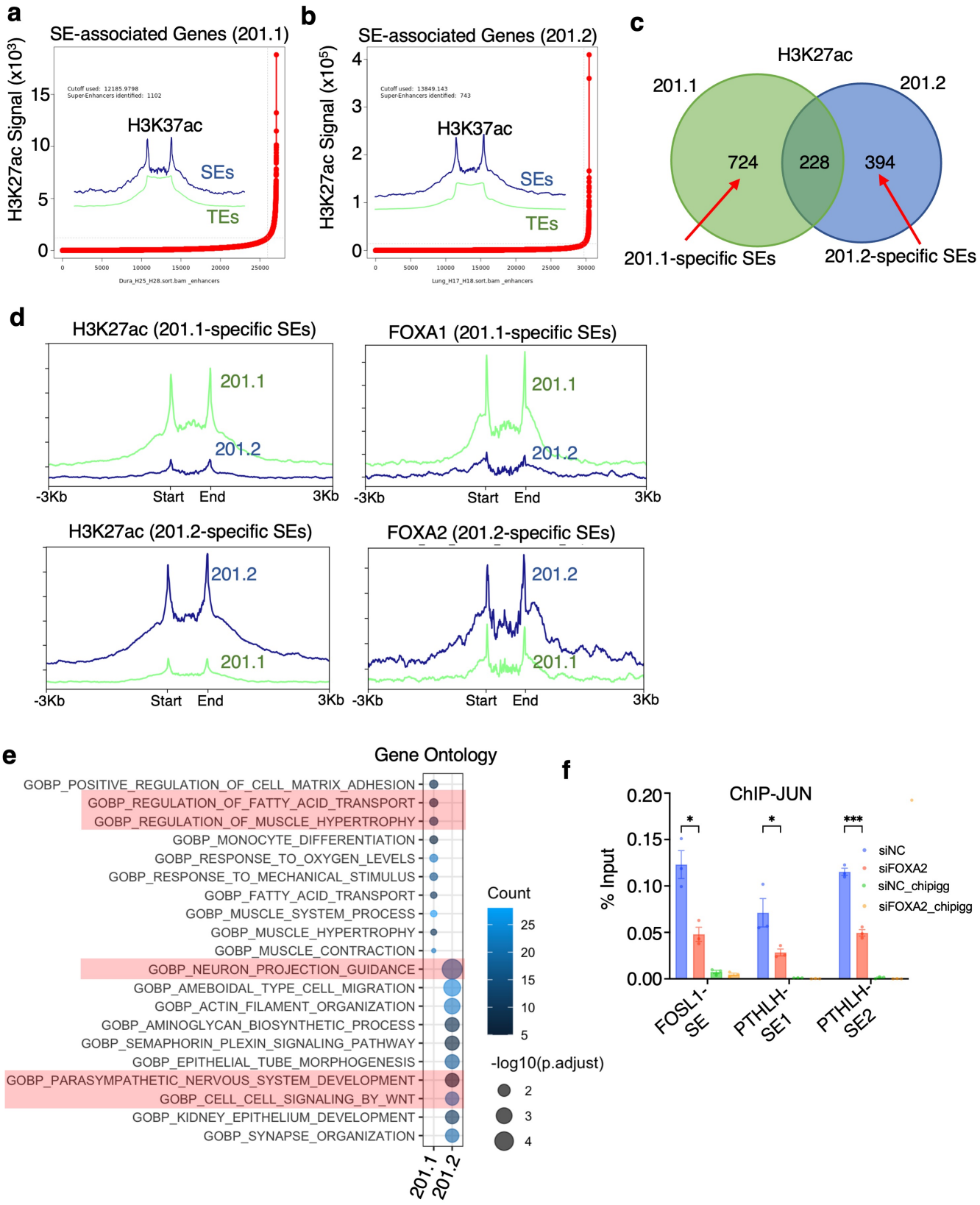

Supplementary Fig. 11| Identification of super-enhancers in PDX models

a, **b**, Model-specific super-enhancers (SEs) were identified using the ROSE algorithm based on ChIP-seq data

for H3K27ac in 201.1 (a) and 201.2 (b) models. **c,** Venn diagram for the overlap of SEs identified in 201.1 and 201.2 models. **d,** Average binding intensities of indicated proteins at 201.1-specific SEs and 201.2-specific SEs in 201.1 and 201.2 models. **e,** Gene ontology annotation analysis to examine the functional enrichment of differential SE-associated genes identified in 201.1 and 201.2 models. **f,** ChIP-qPCR for JUN binding at three SE sites in PC-3 cells transfected with siNTC or siFOXA2 (n=3 independent samples; data represented as mean ± SEM; statistical significance determined by unpaired two-sided *t*-test). ns ($P>0.05$), * ($0.01<P<0.05$), ** ($0.001<P<0.01$), *** ($P<0.001$), and **** ($P<0.0001$) were used to indicate the levels of *P*-value. Source data are provided as a Source Data file.

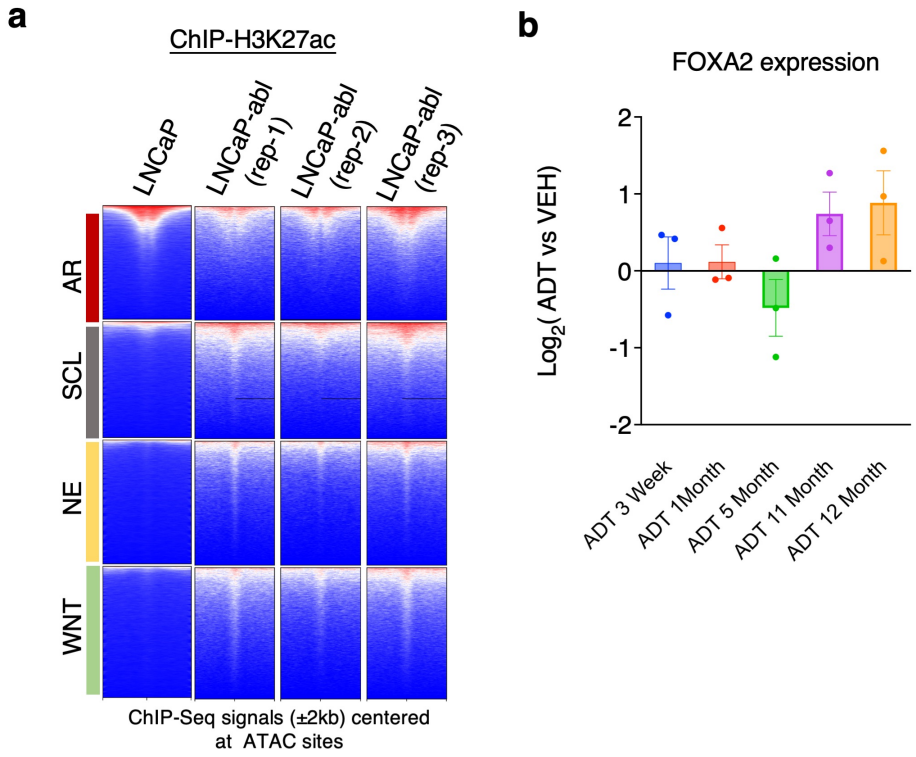

Supplementary Fig. 12| AR targeting treatments drive tumor cells into a multilineage transition state

a, Heatmap view for H3K27ac signal levels at four lineage-specific signature sites in LNCaP and LNCaP-abl cells (continuously cultured in hormone-depleted medium) using public ChIP-seq dataset (GSE114268 [3], GSE72467 [4]). **b**, FOXA2 expression in LNCaP cells cultured in hormone-depleted medium for indicated time points using public dataset (GSE8702 [5]) (Box plot - center: median; box: 25th to 75th IQR; whiskers: 1.5x IQR; outliers: individual data points, n=3 independent samples).

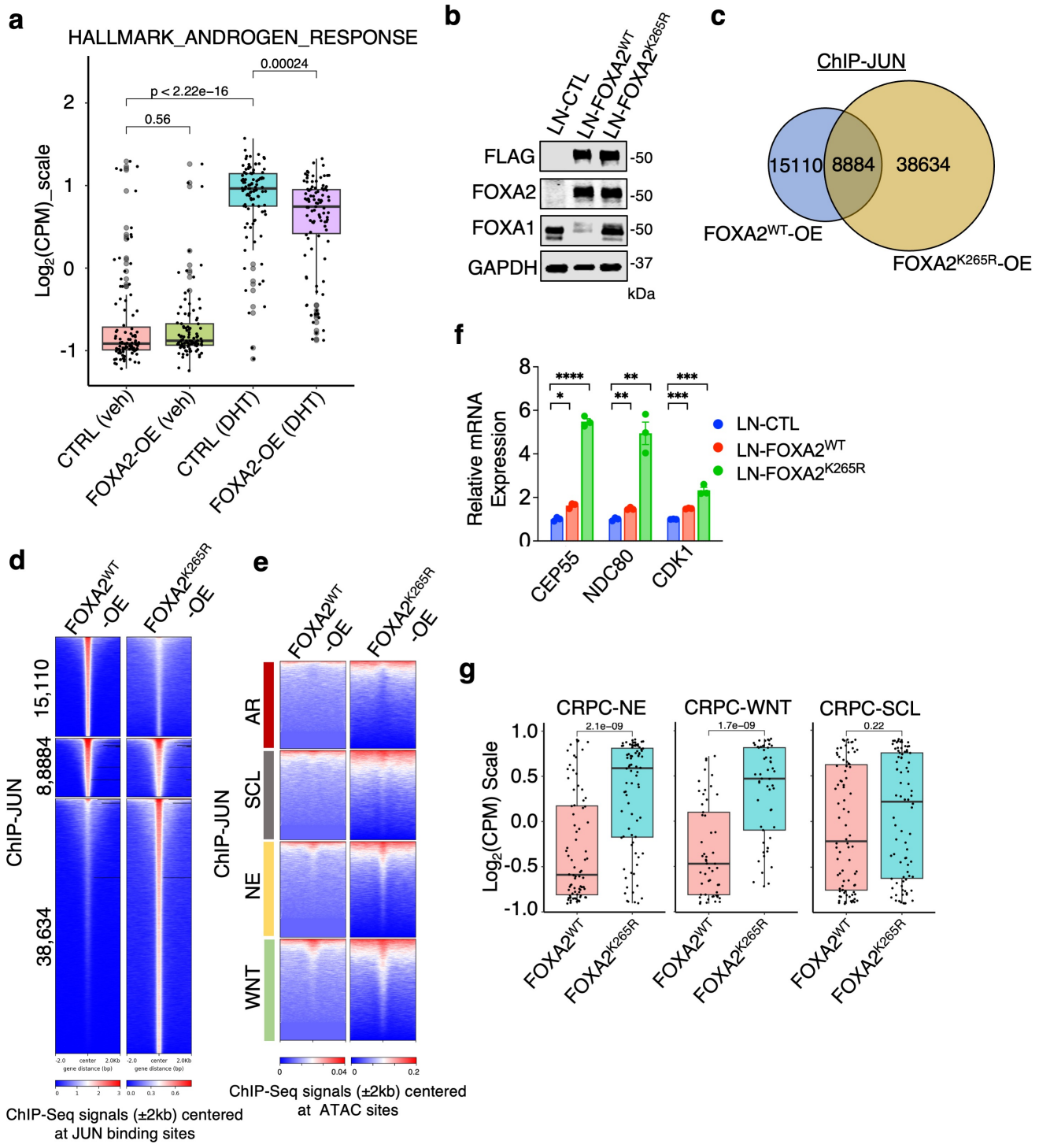

Supplementary Fig. 13| K265R mutation of FOXA2 enhances JUN chromatin binding and maintains the multilineage state of tumor cells

a, Boxplots (center: median; box: 25th to 75th IQR; whiskers: 1.5x IQR; outliers: individual data points; statistical significance determined by unpaired two-sided *t*-test) for expression levels of HALLMARK_ANDROGEN-

_RESPONSE gene set (n=100 genes) in control LNCaP cells or LN-FOXA2-OE cells treated with vehicle or 10nM DHT for 24 hours (based on RNA-seq data). **b**, Immunoblotting for indicated proteins in LNCaP cells overexpressing FLAG-tagged WT FOXA2 or K265R mutant (n=3 independent experiments). **c**, **d**, Venn diagram (c) or heatmap view (d) for JUN ChIP-seq peaks in the WT and K265R cell lines. **e**, Heatmap view for the ChIP-seq signal of JUN centered at specific chromatin sites exhibiting different ATAC signatures for CRPC subtypes [1]. **f**, qRT-PCR for indicated FOXA2/JUN targets in the WT and K265R cell lines (n=3 independent samples; data represented as mean ± SEM; statistical significance determined by unpaired two-sided *t*-test). **g**, Box plots (center: median; box: 25th to 75th IQR; whiskers: 1.5x IQR; outliers: individual data points; statistical significance determined by unpaired two-sided *t*-test) for three non-AR subtype-specific transcriptional signatures (n=93 genes for each subtype [1]) in the WT-expressing cells versus K265R mutant-expressing cells. ns ($P>0.05$), * ($0.01<P<0.05$), ** ($0.001<P<0.01$), *** ($P<0.001$), and **** ($P<0.0001$) were used to indicate the levels of *P*-value. Source data are provided as a Source Data file.

OTHER SUPPLEMENTARY INFORMATION

ChIP-qPCR Primers:

Targets	Sequence (5'->3')
INCENP-F	TGTTGGCTAGAAGGCAAAGGAA
INCENP-R	CCAGTTTTCATCTGCTTTGGGT
CEP55-F	GAGAGCTGCCTGGCTTTTTA
CEP55-R	TGGCATCTTGTGTATCCATGTTTG
ERCC6L-F	CACACACCAGCCTGAGAGAAT
ERCC6L-R	GCTGGGTCTTAGGGAATGTGT
CCBE1_F	AGCTGTTTACTTTTTCATCCCGC
CCBE1_R	GGACCGGAGCTCCTTTTGTG
CDK1_62561458-F	AAAACAGCCTTCCAGGGAGTG
CDK1_62561458-R	ATCCAAGTCAAAGGTAGCTGGA
NDC80-F	GCCATGAGTCACAGAAGGTTG
NDC80-R	TCAGTGATAACCATACCAAACTGG
TP63_F	ACTCATCTGTTTACCTTTTGCTGT
TP63_R	TGTGGTTCTGAGGCTGAGTG
WNT7A_F	GCGTCAGTGAATGGTTGCTG
WNT7A_R	AAACTGGTTCCTGCCATCAG
PTHLH_F_SE1	TGAGAGTTCAATGTTGCGAGTG
PTHLH_R_SE1	TGATTTAACGTCAGGTGTGTGGT
PTHLH_F_SE2	GGGTAGGGGAGGTGCATTTT
PTHLH_R_SE2	TGTGTTGAGCCAGATACTATGTCA
FOSL1_F_SE	CAGGAGTGGGATGAAACGCC
FOSL1_R_SE	TGGGTGGGGTGGTTTATTGG
Mmp3_F	TTATTGACAGTGCAGACGGTCC
Mmp3_R	CTAGCCCAAGGCTTTTCAGGA
Mmp13_F	CCTTCGCCTCACTAGGAAGTT
Mmp13_R	CCCAGGGCAAGCATCTTCTAT

Mutagenesis Primers:

FOXA2_K265R	
HmanFOXA2_K265R_Forward	CGCTTCAAGTGCGAGCGGCAGCTGGCGCTGAA
HumanFOXA2_K265R_Reverse	TTCAGCGCCAGCTGCCGCTCGCACTTGAAGCG
FOXA2(1-165aa)	
FOXA2_1-165aa_Forward	TAGAAGAGCCCGGGCGATCGCGAA

FOXA2_1-165aa_Reverse	CTTTGCGTGCGTGTAGCTGCGCCT
FOXA2(1-324aa)	
FOXA2_324aa_Forward	TAGAAGAGCCCGGGCGATCGCGAA
FOXA2_324aa_Reverse	GCCCCCTCGCTTGTGCTCCTGG
FOXA2(165-463aa)	
FOXA2_166-463aa_Forward	CCGCCCTACTCGTACATCTCGCTC
FOXA2_166-463aa_Reverse	CATGGTACCGAATTCCTTCAAGCCT

Designed siRNA Sequence:

siLSD1	GACAAGCUGUUCCUAAAGAGAAA

Unprocessed Gel Blots: The unprocessed immunoblotting gel blots for Supplementary Figures are provided in the Source Data file.

SUPPLEMENTARY REFERENCES

1. Tang F*, et al.* Chromatin profiles classify castration-resistant prostate cancers suggesting therapeutic targets. *Science* **376**, eabe1505 (2022).

2. Abida W*, et al.* Genomic correlates of clinical outcome in advanced prostate cancer. *Proc Natl Acad Sci U S A* **116**, 11428-11436 (2019).

3. Gao S*, et al.* Chromatin binding of FOXA1 is promoted by LSD1-mediated demethylation in prostate cancer. *Nat Genet* **52**, 1011-1017 (2020).

4. Wang S*, et al.* Modeling cis-regulation with a compendium of genome-wide histone H3K27ac profiles. *Genome Res* **26**, 1417-1429 (2016).

5. D'Antonio JM, Ma C, Monzon FA, Pflug BR. Longitudinal analysis of androgen deprivation of prostate cancer cells identifies pathways to androgen independence. *Prostate* **68**, 698-714 (2008).